PHYSICAL REVIEW B **78**, 241103(R) (2008)

Highly flexible wide angle of incidence terahertz metamaterial absorber: Design, fabrication, and characterization

Hu Tao,[1] C. M. Bingham,[2] A. C. Strikwerda,[3] D. Pilon,[3] D. Shrekenhamer,[2] N. I. Landy,[2] K. Fan,[1] X. Zhang,[1,*] W. J. Padilla,[2] and R. D. Averitt[3,†]

[1]*Department of Mechanical Engineering, Boston University, 15 Saint Mary's Street, Brookline, Massachusetts 02446, USA*
[2]*Department of Physics, Boston College, 140 Commonwealth Avenue, Chestnut Hill, Massachusetts 02467, USA*
[3]*Department of Physics, Boston University, 590 Commonwealth Avenue, Boston, Massachusetts 02215, USA*

(Received 18 August 2008; revised manuscript received 5 November 2008; published 19 December 2008)

We present the design, fabrication, and characterization of a metamaterial absorber which is resonant at terahertz frequencies. We experimentally demonstrate an absorptivity of 0.97 at 1.6 THz. Importantly, our absorber is only 16 μm thick, resulting in a highly flexible material that, further, operates over a wide range of angles of incidence for both transverse electric and transverse magnetic radiation.

DOI: 10.1103/PhysRevB.78.241103 PACS number(s): 78.20.Ci, 77.22.Ch, 78.47.−p

The initial impetus driving metamaterial (MM) research was the realization that a negative refractive index $n(\omega)=\sqrt{\epsilon(\omega)\mu(\omega)}$ could be obtained by creating subwavelength composites where the effective permittivity $\epsilon(\omega)$ and effective permeability $\mu(\omega)$ are independently specified.[1–3] Additionally, metamaterials allow for tailoring the impedance $Z(\omega)=\sqrt{\mu(\omega)/\epsilon(\omega)}$ in a manner not easily achieved with naturally occurring materials. This approach to engineering $n(\omega)$ and $Z(\omega)$ offers unprecedented opportunities to realize electromagnetic responses from the microwave through the visible. This includes cloaks, concentrators, modulators, and spoof plasmons, with many more examples certain to be discovered in the coming years.[4–9]

Quite recently, there has been considerable interest in creating resonant metamaterial absorbers which, through judicious design of $n(\omega)$ and $Z(\omega)$, offer the potential for near-unity absorption.[10–12] The idea is to minimize the transmission and to simultaneously minimize, through impedance matching, the reflectivity. This has been experimentally demonstrated at microwave and terahertz frequencies.[10–12] Other approaches have been theoretically put forward to extend these ideas to higher frequencies or to increase the range of angles of incidence over which the absorptivity remains sufficiently large for applications.[13–15]

While the idea of designing a resonant absorber could be of potential use throughout the electromagnetic spectrum, this concept is expected to be especially fruitful at terahertz frequencies where it is difficult to find strong absorbers. Such absorbers would clearly be of use for thermal detectors or as a coating material to mitigate spurious reflections using continuous-wave sources such as quantum cascade lasers.[10,11,16,17] Progress has been promising where the initial design yielded an absorptivity of 0.70 at 1.3 THz.[11] This work has been extended to a polarization insensitive design with a demonstrated absorptivity of 0.65 at 1.15 THz.[12]

In this Rapid Communication, we experimentally demonstrate a resonant metamaterial with an absorptivity of 0.97 at 1.6 THz. In comparison to previous designs,[11,12] the current design has several important advantages. Most importantly, the present design is on a highly flexible polyimide substrate with a total thickness of 16 μm thick which enables its use in nonplanar applications as it can easily be wrapped around objects as small as 6 mm in diameter. In addition, we demonstrate, through simulation and experiment, that this metamaterial absorber operates over a very wide range of angles of incidence for transverse electric (TE) and transverse magnetic (TM) configurations. Finally, the bottom layer of the absorber consists of a continuous metal film which simplifies the fabrication in that, for this two-layer structure, precise alignment between the layers is not required.

Maximizing the absorption A is equivalent to minimizing both the transmission T and reflectivity R in that $A=1-T-R$. As has been demonstrated,[12] in the limit that impedance matching to free space is achieved (i.e., $Z=Z_0$ resulting in $R=0$), the transmission reduces to $T=\exp(-2n_2dk)=\exp(-\alpha d)$, where k is the free space wave vector, d is the sample thickness, n_2 is the imaginary part of the refractive index, and α is the absorption coefficient. Thus, impedance matching is a crucial step yielding a transmission that is determined solely by the losses in the slab of thickness d. In the case of a metamaterial absorber the effective n_2 is determined by $\epsilon(\omega)$ and $\mu(\omega)$. Thus, the design of a near-unity resonant metamaterial absorber $\epsilon(\omega)$ and $\mu(\omega)$ must be optimized such that, at the desired center frequency, $Z=Z_0$ with n_2 as large as possible. The absorption ultimately arises from losses within the metal and dielectric slab.

A compact metamaterial absorber consists of two metallic layers separated by a dielectric spacer. The top layer consists of an array of split ring resonators (SRR) which is primarily responsible for determining $\epsilon(\omega)$, while the bottom metallic layer is designed such that the incident magnetic field drives circulating currents between the two layers. However, given the strong coupling between the two layers, fine tuning of the geometry is required to obtain the conditions described in the previous paragraph. Fortunately, using full-wave electromagnetic simulation, rapid convergence to a near optimal design is readily achieved.

Figure 1 presents such an optimized design which we have subsequently fabricated and tested. The top layer [Fig. 1(a)] consists of an array of 200-nm-thick Au electrically resonant split ring resonators,[18,19] with the dimensions listed in the figure caption. In the absence of a second metallic layer, this structure displays two resonances.[18,19] The lowest-

 ©2008 The American Physical Society

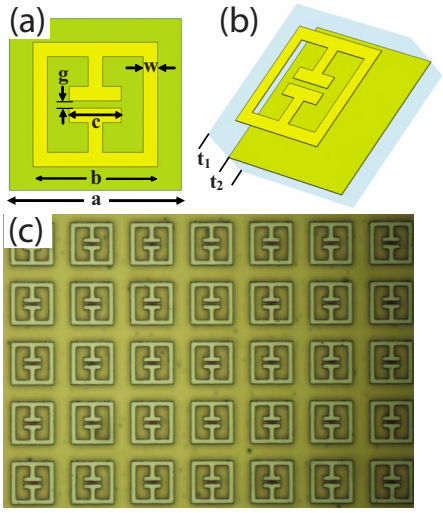

FIG. 1. (Color online) Terahertz metamaterial absorber consisting of two metallic layers and two dielectric layers. (a) Electric SRR: unit-cell a: 36 μm, SRR side length b: 25.9 μm, capacitor length c: 10.8 μm, capacitor gap g: 1.4 μm, and linewidth w: 3 μm. (b) Perspective view of the absorber. Each dielectric layer, t_1 and t_2, is 8 μm thick. (c) Photograph of a portion of the experimentally realized absorber.

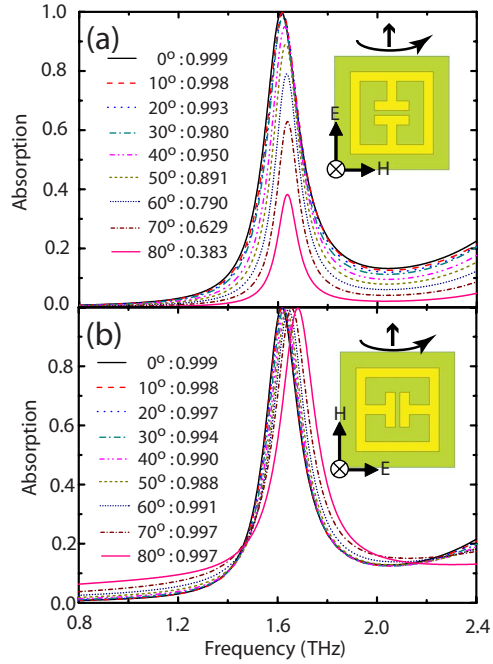

FIG. 2. (Color online) Simulations of the metamaterial absorber showing the absorptivity as a function of frequency at various angles of incidence for (a) TE and (b) TM incident radiation. The insets depict the orientation of the fields with respect to the SRR. The labels for the curves show the angle of incidence and the corresponding peak absorptivity.

frequency resonance is an LC response with the inductance given by the two loops on either side of the center capacitor. This resonance is only driven when the electric field is perpendicular to the capacitor plates (see insets of Fig. 2). There is also a higher-frequency resonance associated with a dipolar response from the two side bars. While both contribute to the effective $\epsilon(\omega)$, the LC resonance, as will be discussed in more detail below, is critical in creating a resonant absorber. A dielectric spacer layer of 8 μm thick separates this top layer from the bottom metallic layer. The bottom metallic layer is a continuous 200-nm-thick Au film. As Fig. 1(b) shows, there is a second 8-μm-thick dielectric layer which provides mechanical support but, being behind the continuous Au film, does not contribute to the electromagnetic response. Figure 1(c) shows a photograph of a portion of the structure we have fabricated and tested as detailed below.

The optimized structure presented in Fig. 1 was obtained through computer simulations using the commercial program CST Microwave Studio™ 2006B.04. The frequency domain solver was utilized where the Au portions of the metamaterial absorber were modeled as lossy gold with a frequency-independent conductivity $\sigma=4.09\times10^7$ S/cm. The 8-μm-thick dielectric layer was modeled using the experimentally measured value of polyimide as this is what is used in the subsequent fabrication. Specifically, a frequency independent $\tilde{\epsilon}=\epsilon_1+i\epsilon_2=2.88+i0.09$ was used which corresponds to a loss tangent $\tan(\delta)=\epsilon_2/\epsilon_1=0.0313$.[20] The amplitudes of the transmission S_{21} and reflection S_{11} were obtained, and the absorption was calculated using $A=1-R-T=1-S_{11}^2-S_{21}^2$ where, as expected for the present design, S_{21} is zero across the entire frequency range due to the ground plane. The optimized structure presented in Fig. 1 was obtained (simulating radiation at normal incidence) through parameter sweeps of the dimensions of the SRR and the dielectric spacer thickness. The optimized parameters are those which yielded the lowest reflectivity at the design frequency of 1.6 THz.

The simulated absorption as a function of frequency for the optimized structure (Fig. 1) is presented in Fig. 2 for TE [Fig. 2(a)] and TM [Fig. 2(b)] radiation at various angles of incidence. For the TE case, at normal incidence a peak absorption of 0.999 is obtained. With increasing angle of incidence, the absorption remains quite large and is at 0.89 at 50°. Beyond this there is a monotonic decrease in the absorption as the incident magnetic field can no longer efficiently drive circulating currents between the two metallic layers. There is also a slight frequency shift of ~30 GHz from 0° to 80°. For the case of TM radiation shown in Fig. 2(b), the absorption at normal incidence is 0.999 and remains greater than 0.99 for all angles of incidence. In this case, the magnetic field can efficiently drive the circulating currents at all angles of incidence which is important to maintain impedance matching. The frequency shift for TM radiation is ~80 GHz from 0° to 80°. As these simulations reveal, this MM absorber operates quite well for both TE and TM radiation over a large range of angles of incidence.

To better understand the nature of this absorption, in Fig. 3 we present the simulated absorption over a broader frequency range. The black curve reveals that, in addition to the strong absorption at 1.6 THz, there is a secondary absorption at approximately 2.8 THz. The calculated surface current densities in the top resonator structure and the lower ground plane for the 1.6 and 2.8 THz resonances are displayed below the absorption and labeled as I and II, respectively. For the 1.6 THz resonance, it is evident that in the plane of the

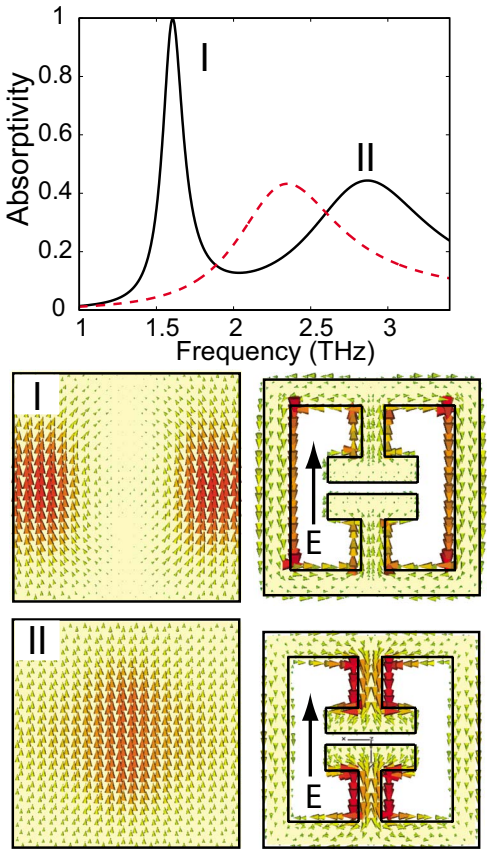

FIG. 3. (Color online) The simulated absorption (for normal incidence) out to 3.5 THz revealing an additional absorption. The middle panel shows the calculated surface current density for the low-frequency absorption, while the lower panel shows the calculated surface current density for the higher-frequency resonance. The red dashed curve shows the absorption with the capacitor shorted highlighting the importance of the in-plane electric response in determining the low-frequency absorption.

electric resonator there are countercirculating currents which are associated with the *LC* resonance mentioned previously. In addition, there is also a magnetic response associated with a circulating displacement current between the resonator and the ground plane. In contrast, the 2.8 THz resonance is determined solely by the magnetic response which drives the circulating displacement current between the resonator and ground plane. This high-frequency response is analogous to what has previously been observed using frequency-selective surfaces at microwave frequencies,[21,22] while the lower-frequency resonance takes advantage of the resonant in-plane frequency response which has not previously been considered. This is further highlighted by the red curve which shows the calculated absorption if the capacitor is shorted. The low-frequency response vanishes while the higher-frequency resonance remains, albeit shifted to a slightly lower frequency. Interestingly, the low-frequency response has a higher Q and, occurring at a longer wavelength, is further in the effective-medium regime.

An additional aspect to consider in the design of metamaterial absorbers is losses in the constituent materials comprising the structure. As discussed above, one of the design criteria is to obtain a large value of the imaginary part of the effective refractive index. This necessitates having losses in the metal and/or the dielectric spacer. For example, in the limit of a perfect electric conductor and a lossless dielectric, the absorption in the composite in Fig. 1 is zero. However, the losses in gold are sufficient to yield a strong narrow-band resonance as shown in Figs. 2 and 3.

The metamaterial absorber structures were fabricated with a surface micromachining process on flexible polyimide substrate using a silicon wafer as the supporting substrate during the fabrication process. Liquid polyimide (PI-5878G, HD MicroSystems™) was spin coated on a 2 in. silicon wafer to form the freestanding substrate. In this work, the polyimide was spin coated at 1700 rpm and cured for 5 h in an oven at 350 °C in a nitrogen environment yielding an 8-μm-thick polyimide layer. A 200-nm-thick Au/Ti film was e-beam evaporated on the polyimide substrate to form the ground plane. Another 8-μm-thick polyimide layer was spin coated on the top of the ground plane to form the polyimide spacer and processed according to the procedure mentioned above. For the SRR array, direct laser writing technology was chosen over traditional mask contact lithography technology to improve the patterning quality on the polyimide substrates. Shipley™ S1813 positive photoresist was first calibrated and then exposed with a Heidelberg™ DWL 66 laser writer to pattern the top layer of electric ring resonators. Another 200-nm-thick Au/Ti film was e-beam evaporated followed by rinsing in acetone for several minutes. The metamaterial absorber fabricated on the polyimide substrate was carefully peeled off of the silicon substrate at the end of fabrication. Our samples show significant mechanical flexibility and can be easily wrapped around a cylinder with a radius of a few millimeters.

A Fourier transform infrared (FTIR) spectrometer was used to experimentally verify the behavior of the absorber by measuring the transmission and reflection over the frequency range of 0.6–3 THz with a resolution of 15 GHz. A liquid-helium-cooled bolometer detector and germanium coated 6 μm Mylar beam splitter were used to optimize the FTIR performance over the frequencies measured. Prior to measurement, the absorber samples were diced into 1×1 cm^2 squares. The aperture of the incident beam was 5 mm, which is considerably smaller than the sample dimension. The sample was mounted at normal incidence for the transmission measurement. As expected, the transmitted intensity was essentially zero due to the gold ground plane which blocks all radiation through the absorber. The achievable incident angle for reflection measurements is constrained within the range of 30–60 off normal due to the experimental limitations. The measurements were performed with electric field perpendicular to the SRR gap to excite the electric resonance. The absorption spectrum was easily obtained from the reflection results (i.e., $A=1-R$).

The experimental results are displayed in Figs. 4(a) and 4(b) for TE and TM incident radiation, respectively. For the TE radiation, the absorption peaks at 0.95 for an angle of incidence of 30° decreasing slightly to 0.88 at 60°. This is in reasonable agreement with the simulations though the experimental absorptivity at 60° is ~0.09 higher than for simulation. However, the off-resonance absorptivity is quite large

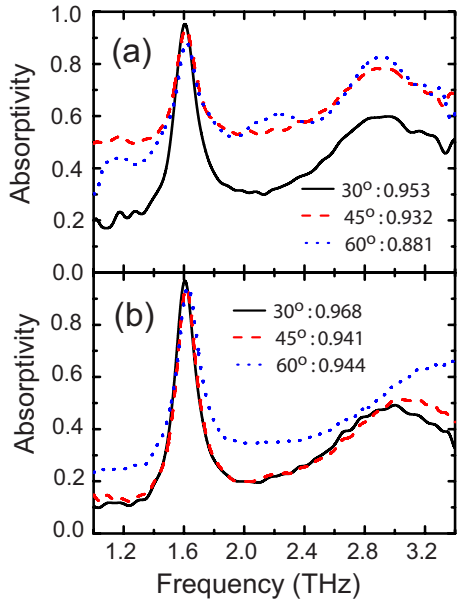

FIG. 4. (Color online) Experimentally measured absorption as a function of frequency for (a) TE and (b) TM radiation at 30°, 45°, and 60° angles of incidence.

in disagreement with the simulations. This may arise, in part, from scattering of radiation from imperfections arising from the fabrication. For the TM measurements the peak absorptivity is 0.968 at 30° angle of incidence and only drops by 0.024 upon increasing to 60°. Further, the increase in the baseline absorption is much smaller in comparison to the TE measurements and is in better agreement with simulations. A closer inspection of Fig. 4(b) also reveals a slight increase in the resonance frequency with increasing angle of incidence in agreement with simulation. We also note that the higher-frequency resonance as discussed in the context of Fig. 3 is also observed. Overall, these results substantially confirm the simulation results demonstrating that our MM absorber yields a large absorptivity over a broad range of angles of incidence for both TE and TM radiation.

In summary, we have presented the design, fabrication, and characterization of a highly flexible metamaterial absorber that, experimentally, obtains an absorptivity of 0.96 at 1.6 THz and, further, operates over a wide angular range for TE and TM radiation. Such a composite terahertz metamaterial may find numerous applications ranging from the active element in a thermal detector to terahertz stealth technology.

We acknowledge partial support from the Los Alamos National Laboratory LDRD program, DOD/Army Research Laboratory under Contract No. W911NF-06-2-0040, NSF under Contract No. ECCS 0802036, and DARPA under Contract No. HR0011-08-1-0044. The authors would also like to thank the Photonics Center at Boston University for all of the technical support throughout the course of this research.

*xinz@bu.edu
†raveritt@physics.bu.edu

[1] D. R. Smith, W. J. Padilla, D. C. Vier, S. C. Nemat-Nasser, and S. Schultz, Phys. Rev. Lett. **84**, 4184 (2000).
[2] V. G. Veselago, Sov. Phys. Usp. **10**, 509 (1968).
[3] R. A. Shelby, D. R. Smith, and S. Schultz, Science **292**, 77 (2001).
[4] D. Schurig, J. J. Mock, B. J. Justice, S. A. Cummer, J. B. Pendry, A. F. Starr, and D. R. Smith, Science **314**, 977 (2006).
[5] J. B. Pendry, D. Schurig, and D. R. Smith, Science **312**, 1780 (2006).
[6] M. Rahm, S. A. Cummer, D. Schurig, J. B. Pendry, and D. R. Smith, Phys. Rev. Lett. **100**, 063903 (2008).
[7] W. J. Padilla, A. J. Taylor, C. Highstrete, Mark Lee, and R. D. Averitt, Phys. Rev. Lett. **96**, 107401 (2006).
[8] H.-T. Chen, W. J. Padilla, J. M. O. Zide, A. C. Gossard, A. J. Taylor, and R. D. Averitt, Nature (London) **444**, 597 (2006).
[9] F. J. Garcia-Vidal, L. Martin-Moreno, and J. B. Pendry, J. Opt. A, Pure Appl. Opt. **7**, S97 (2005).
[10] N. I. Landy, S. Sajuyigbe, J. J. Mock, D. R. Smith, and W. J. Padilla, Phys. Rev. Lett. **100**, 207402 (2008).
[11] H. Tao, N. I. Landy, C. M. Bingham, X. Zhang, R. D. Averitt, and W. J. Padilla, Opt. Express **16**, 7181 (2008).
[12] N. I. Landy, C. M. Bingham, T. Tyler, N. Jokerst, D. R. Smith, and W. J. Padilla, arXiv:0807.3390 (unpublished).
[13] M. Diem, T. Koschny, and C. M. Soukoulis, arXiv:0807.2479 (unpublished).
[14] I. Puscasu and W. L. Schaich, Appl. Phys. Lett. **92**, 233102 (2008).
[15] Y. Avitzour, Y. A. Urzhumov, and G. Shvets, arXiv:0807.1312 (unpublished).
[16] G. P. Williams, Rep. Prog. Phys. **69**, 301 (2006).
[17] M. Tonouchi, Nat. Photonics **1**, 97 (2007).
[18] D. Schurig, J. J. Mock, and D. R. Smith, Appl. Phys. Lett. **88**, 041109 (2006).
[19] W. J. Padilla, M. T. Aronsson, C. Highstrete, M. Lee, A. J. Taylor, and R. D. Averitt, Phys. Rev. B **75**, 041102(R) (2007)
[20] H. Tao, A. C. Strikwerda, K. Fan, C. M. Bingham, W. J. Padilla, X. Zhang, and R. D. Averitt, J. Phys. D: Appl. Phys. **41**, 232004 (2008).
[21] D. F. Sievenpiper, L. Zhang, R. F. Jimenez Broas, N. G. Alexopolous, and E. Yablonovitch, IEEE Trans. Microwave Theory Tech. **47**, 2059 (1999).
[22] J. M. Hao, L. Zhou, and C. T. Chan, Appl. Phys. A: Mater. Sci. Process. **87**, 281 (2007).